Magazine of Civil Engineering

ISSN 2071-0305

journal homepage: http://engstroy.spbstu.ru/

DOI: 10.18720/MCE.94.8

Behavior of strengthened concrete beams damaged by thermal shock

R. Al-Rousan*

Jordan University of Science and Technology, Irbid, Jordan

** E-mail: rzalrousan@just.edu.jo*

Keywords: reinforced concrete, thermal shock, structural strength, shear, flexural strength, fiber reinforced polymer, nonlinear, finite element analysis

Abstract. In the last two decades, using of Carbon Fiber Reinforced Polymers (CFRP) in strengthening of deficient reinforced concrete structural elements has been increased due to their ease of installation, low invasiveness, high corrosion resistance, and high strength to weight ratio. Strengthening damage structures is a relatively new technique. The aims of this study is to investigate the effectiveness of using CFRP to regain shear capacity of shear-deficient reinforced concrete (RC) beams after being damaged by thermal shock. Firstly, a novel Nonlinear Finite Element Analysis (NLFEA) model is created and validated. Then, Ten RC beams (100×150×1400 mm) have been constructed and divided into two groups to scrutinize the effect of CFRP strip number and thermal shock impact. The performance of each beam was evaluated in terms of failure mode, CFRP strain, load-deflection behavior, ultimate deflection, ultimate load capacity, elastic stiffness, toughness, performance factor, and profitability Index of the CFRP Strips. Load carrying capacity and stiffness of RC beams decreased about 68 % and 71 %, respectively, as compared with reference un-damaged beam. Strengthening the thermal damaged RC beams allowed recovering the original load carrying without achieving the original stiffness. Strengthened beams with fully CFRP plates regained the original load capacity with a corresponding stiffness from 79 % to 105 %, respectively. Finally, the enhancement percentage increased with the increase of bonded area or number of CFRP strips and these percentages sharply dropped for damaged beams.

1. Introduction

Flexural and shear are the main failure modes of RC beams. Shear failure of RC beams is classified as brittle and occurs unexpectedly without any warning while the flexural failure is ductile. Therefore, it is a necessity to make sure that the shear design of RC beams must be safe in order to develop their full flexural capacity. Unfortunately, many of existing RC beams suffering shear deficiencies due to construction faults, poor construction practices, mistakes in design calculations, changing in structure function, improper detailing of shear reinforcement and steel corrosion. Elevated temperatures cause severe damage for reinforced concrete (RC) structures, such as RC beams. RC beams have been reported to loss strength and stiffness with relatively large permanent deformations because of exposure to high temperatures [1]. These harmful effects could be attributed to the deterioration of mechanical characteristics of concrete and steel rebars and the redistribution of stresses within the beam due to the elevated temperatures [2–17]. Currently, the most commonly used technique to repair the heat-damaged RC beams is using carbon fiber reinforced polymer (CFRP) composites. These sheets are advanced materials that can be easily applied on the structures and characterized by outstanding mechanical and corrosion resistance characteristics. Various studies were performed to investigate the flexural behavior of RC beams wrapped with CFRP. The results showed that externally bonded carbon FRP (CFRP) sheets and laminates has the ability to enhance the flexural behavior of the beams and recover, to certain limit, the flexural strength of heat-damaged beams. Strengthening level or recovery depends on several factors such as degree of beam's damage, geometry and type of fiber sheet, CFRP layers number, and the resin's type and properties [18–33].

Reinforcing concrete structures are often subjected to cycles of heating–cooling such as in chimneys, concrete foundations for launching rockets carrying spaceships, concrete near to furnace, clinker silos and nuclear power plants, or those subjected to fire then extinguished using water. Temperature cycles are critical

Al-Rousan, R. Behavior of strengthened concrete beams damaged by thermal shock. Magazine of Civil Engineering. 2020. 94(2). Pp. 93–107. DOI: 10.18720/MCE.94.8

to the stability of concrete structures and require considerations upon design [34, 35]. As well stipulated, the mechanical properties of concrete are preserved for exposure temperatures below 300 °C, yet are decreased considerably as temperature exceeds 500 °C. Additional damage results from rabid cooling such as in the case of distinguishing of fire with cool water due to creation of temperature gradient between concrete core and its surface. This results in tensile stresses on the concrete surface that are high enough to crack concrete and this considered as another source of damage results from incompatible expansion and contraction of aggregate and surrounding cement paste. The magnitude of damage is influenced by many factors such as the size of concrete members, the type of cement and aggregate, the concrete moisture content and the predominant environmental factors, Those are represented in heating exposure time and rate, type of cooling, and maximum temperature attained [36].

The shear deficient Reinforced concrete (RC) beams may be externally strengthened with bonded fiber reinforced polymer (FRP) composites through bonding on their sides only, U jacketing, or complete wrapping. Debonding and FRP rupture are the main shear failure modes of strengthened beams with FRP [37–46]. Different types of materials and techniques were used in strengthening and retrofitting of existing concrete structures such as steel plates bolting, reinforced concrete jackets, pre-stressed external tendons, and most recently FRP composite which has been used on a large scale in different countries. FRP composites have many advantages over conventional methods represented in ease of application, high strength-to-weight ratio, excellent mechanical strength, and good resistance to corrosion, especially that most structures are damaged due to dynamic loads, corrosion of steel, and freeze-thaw cycles [46, 47].

In the construction industry, there is growing attention of using effective external strengthening techniques such as bonding of CFRP composites onto the external deficient faces of the structural members due to their ease of installation, low invasiveness, high corrosion resistance, and high strength to weight ratio. As a result, the center of consideration of the majority of previously published studies was either only on the impact of fibers on the structural behavior of reinforced concrete elements or using CFRP composite as external strengthening for flexural or shear. The intent was to arrive at the vital CFRP strengthening technique that provides an effective increase in the shear strength while maintaining ductile failure mode. Therefore, essential issues to produce effective, economical, and successful CFRP strengthening were needed. Also, exposure of such beams to thermal shock due to any of the reasons described earlier would aggravate the weakness of the high shear zone that unless otherwise strengthened would cause imminent shear failure. External strengthening with CFRP composites have established itself as an efficient method for strengthening of deficient beams in regaining shear strength, especially when concrete is thermally damaged, has not been well established. The scientific problem considered in the study is indeed one of the problems in the modern theory of deficient reinforced concrete shear beams. A lack of literature regarding behavior of shear deficient beams damaged by thermal shock necessitated conducting the present investigation.

2. Methods

Nonlinear finite element analysis (NLFEA) is an effective and important tool in the analysis of complex structures. The main benefits that NLFEA include: 1) substantial savings in the cost, time, and effort compared with the fabrication and experimental testing of structure elements; 2) allows to change any parameter of interest to evaluate its influence on the structure, such as the concrete compressive strength; 3) allows to see the stress, strain, and displacement values at any location and at any load level. Twenty-six full-scale models strengthened using CFRP are developed to carry out different investigated parameters.

2.1. Experimental Work Review

The validation process of the finite element model is based on the experimental work performed by Haddad and Al-Rousan [48]. Four high strength reinforced concrete (RC) beams (100×150×1400 mm) were designed without shear reinforcement in the shear region. Stirrups were placed only within the constant moment region to allow easier positioning of flexural reinforcement and to provide improved confinement of concrete within the constant moment region, as shown in Figure 1. Steel reinforcement: Grade 60 deformed steel bars of 16 mm diameter were used in the tension zone of the reinforced concrete (RC) beams, a steel bars of 12 mm diameter used as top steel reinforcement, and 8 mm diameter bars were used for stirrups. Unidirectional plates and sheets at a thickness of 1.4 and 0.17 mm and a width of 50 and 500 mm, respectively, were used in repairing of thermally damage RC beams. The tensile strength, modulus of elasticity, and strain at failure for CFRP plate and sheet are (3900 MPa, 2700 MPa), (230000 MPa, 165000 MPa), and (1.5 % and 1.4 %), respectively. RC beam specimens were subjected to heat at 500 °C for about two hours using the electrical furnace before immersion inside the water. Figure 1 shows the configuration of different repair techniques. The RC beams were tested under four-point loading, as shown in Figure 1. The span between the supports was 1300 mm and the distance between two point loads was 300 mm. Table 1 shows the Failure load, maximum CFRP strain, and modes of failure from the tested [48] and NLFEA.

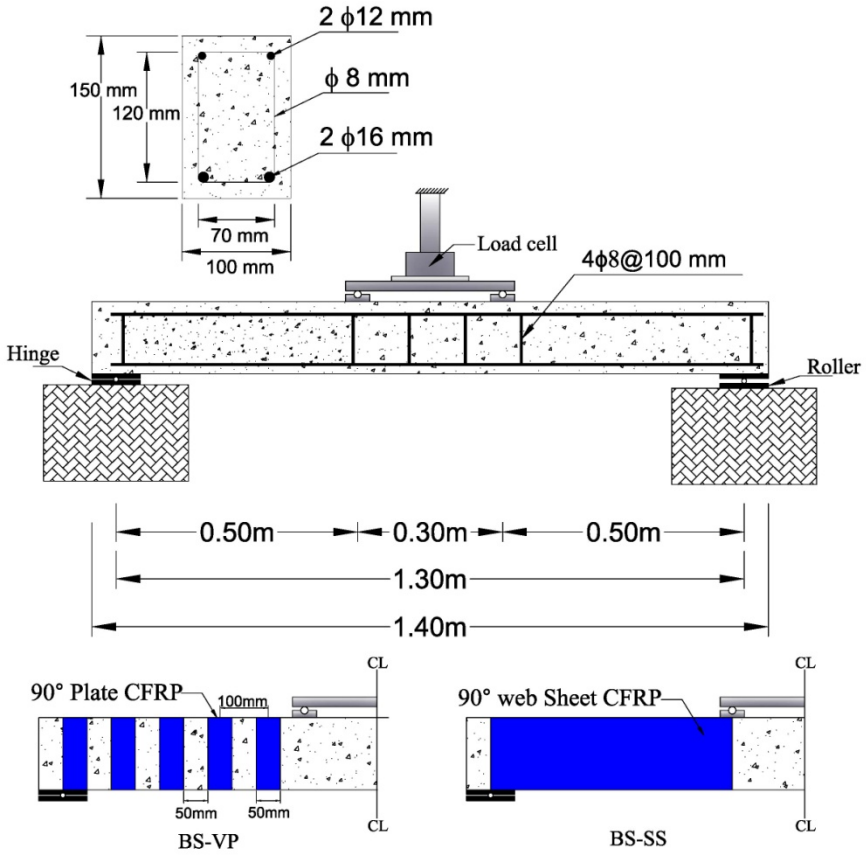

Figure 1. Setup and reinforcement details of the beams [48].

Table 1. Failure load, maximum CFRP strain, and modes of failure.

Specimens	Test/NLFEA	Ultimate Load (kN)	δ_u (mm)	Maximum CFRP strain (ε_{max})	Failure Mode
BC	Experimental	35.2	5.94	N.A	DS
	NLFEA	35.6	4.72	N.A	DS
BC-TD	Experimental	11.3	4.13	N.A	DS
	NLFEA	11.3	4.48	N.A	DS
BS-VP	Experimental	31.7	6.09	13270	DS
	NLFEA	32.1	6.23	13274	DS+LDP
BS-SS	Experimental	35.9	5.81	11700	DS
	NLFEA	37.3	6.84	14540	DS+LDP

Note: DS: diagonal shear; LDP Local debonding.

2.2. Description of Non-linear Finite Element Analysis (NLFEA)

Concrete is non-homogenous and brittle material and has different behavior in tension and compression. SOLID 65 element is capable to predict the nonlinear behavior of concrete materials by using a smeared crack approach by ultimate uniaxial tensile and compressive strengths. The average compressive strength of the cylinders before and after being damaged by thermal shock were 53.5 and 9.8 MPa, respectively, and the average splitting tensile strength of the cylinders before and after being damaged by thermal shock were 2.9 and 0.7 MPa, respectively. Poisson's ratio of 0.2 and shear transfer coefficient (β_t) of 0.2 for β_t was used in this study. Figure 14(a) shows the stress-strain relationship for unconfined concrete which describes the post-peak stress-strain behavior.

The steel in simulated models was assumed to be an elastic-perfectly plastic material and the same in compression and tension. Poisson's ratio of 0.3 and the yield stress of undamaged and damaged beams were 420 MPa and $0.78f_y$ [49], respectively, as well as the elastic modulus were 200 GPa and $0.6E_s$ [49], respectively, were used for the steel reinforcement. Figure 2(b) shows the idealized stress-strain relationship. The steel plates were assumed to be linear elastic materials with a Poisson ratio and elastic modulus of 0.3 and 200 GPa, respectively. The CFRP sheet is assumed to be an orthotropic material 0.17 mm thick, tensile strength of 3900 MPa, elastic modulus of 230 GPa, and ultimate tensile strain of 0.0169 as shown in Figure 2(c).

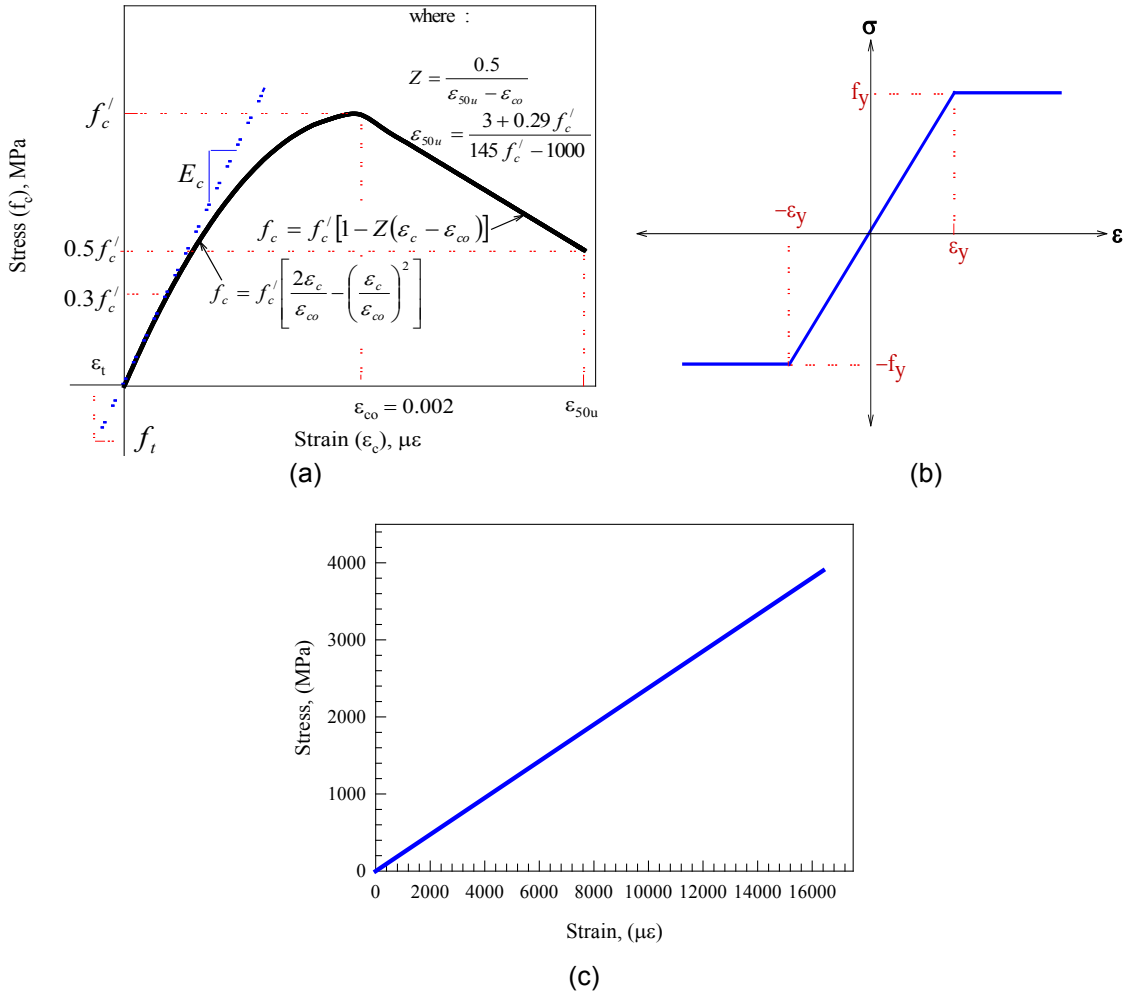

Figure 2. Stress-strain curves for: (a) unconfined concrete [48], (b) steel reinforcement [49], and CFRP composite.

The contact area between the concrete and CFRP composite was modeled by a CONTA174 element. In this study, the bond stress-slip model between CFRP plates and damaged concrete by thermal shock proposed by Haddad and Al-Rousan [50] was used as shown in Figure 3. Figure 4 shows a typical finite element meshing of all beams. The total load applied was divided into a series of load increments or load steps. Newton-Raphson equilibrium iterations provide convergence at the end of each load increment within tolerance limits equal to 0.001 with load increment of 0.35 kN.

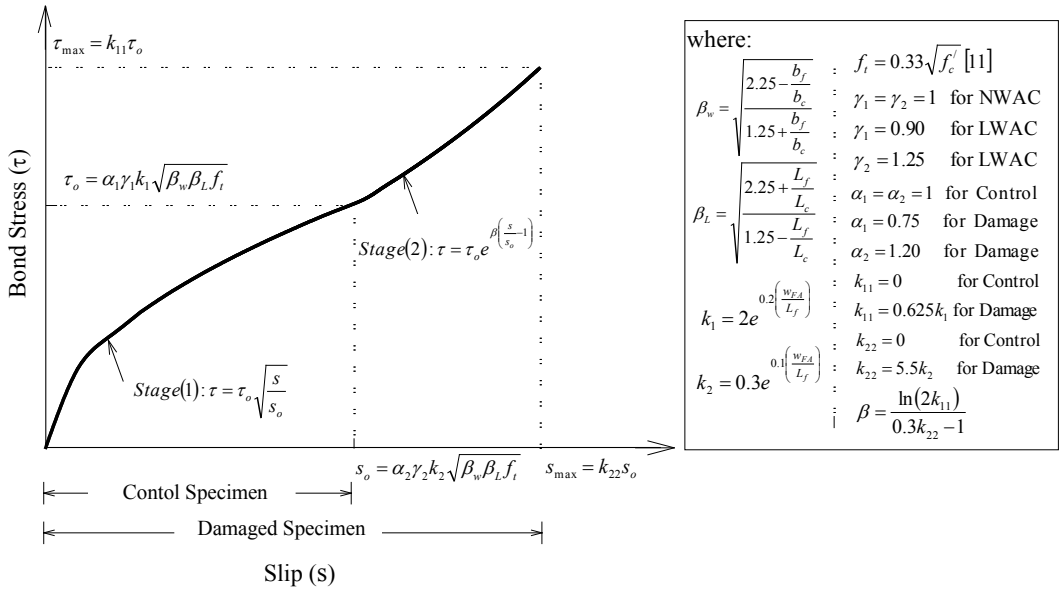

Figure 3. CFRP to concrete bond slip model [50].

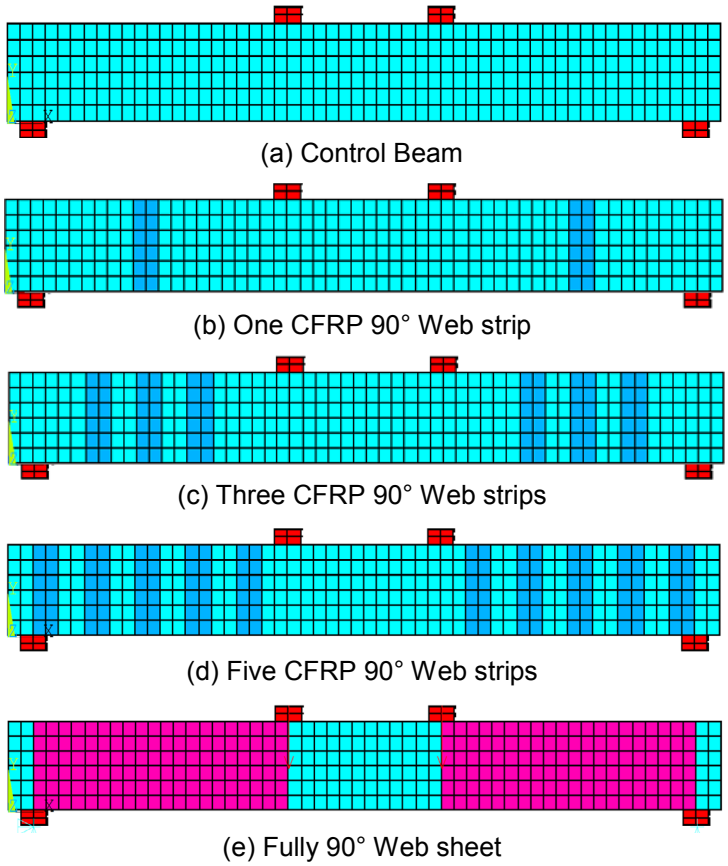

Figure 4. Typical finite element meshing of the beams.

2.3. Investigated Parameters

Figure 4 shows the configuration of different strengthening techniques, where unlike one un-damaged control beam (BC-UD) and one control damaged beam (BC-D), and the other eight beams were strengthened in shear using CFRP sheets as follows: BS1-UD and BS1-D (undamaged and damaged, respectively) were strengthened using one vertical strip (50 mm wide × 0.17 mm thick) on both sides within the constant shear zone of 500 mm. BS3-UD and BS3-D (undamaged and damaged, respectively) were strengthened using three vertical strip (50 mm wide × 0.17 mm thick), spaced at 100 mm center to center on both sides within the constant shear zone of 500 mm. BS5-UD and BS5-D (undamaged and damaged, respectively) were strengthened using five vertical strip (50 mm wide × 0.17 mm thick) on both sides within the constant shear zone of 500 mm. BSS-UD and BSS-D (undamaged and damaged, respectively) were strengthened using sheet to the web sides only (500 mm wide × 0.17 thick) on both sides within the constant shear zone of 500 mm. A full description of the finite element modeling groups is shown in Table 2.

Table 2. Investigated parameters.

Group Number	Beam number	Un-damaged/ Damaged	CFRP strengthening configuration
1	BC-UD	Un-damaged	Control beam without strengthening
	BS1-UD		One vertical strip (50 mm wide × 0.17 mm thick) on both sides within the constant shear zone of 500 mm.
	BS3-UD		Three vertical strip (50 mm wide × 0.17 mm thick), spaced at 100 mm center to center on both sides within the constant shear zone of 500 mm
	BS5-UD		Five vertical strip (50 mm wide × 0.17 mm thick), spaced at 100 mm center to center on both sides within the constant shear zone of 500 mm
	BSS-UD		Fully sheet to the web sides only (500 mm wide × 0.17 thick) on both sides within the constant shear zone of 500 mm
2	BC-D	Damaged	Control beam without strengthening
	BS1-D		One vertical strip (50 mm wide × 0.17 mm thick) on both sides within the constant shear zone of 500 mm.
	BS3-D		Three vertical strip (50 mm wide × 0.17 mm thick), spaced at 100 mm center to center on both sides within the constant shear zone of 500 mm
	BS5-D		Five vertical strip (50 mm wide × 0.17 mm thick), spaced at 100 mm center to center on both sides within the constant shear zone of 500 mm
	BSS-D		Fully sheet to the web sides only (500 mm wide × 0.17 thick) on both sides within the constant shear zone of 500 mm

Note: B: Beam, UD: un-damaged, D: Damaged, S1: one vertical sheet, S3: three vertical sheets, S5: five vertical sheets, SS: fully sheet.

2.4. Validation Process

Four beams were simulated to validate the NLFEA of the reinforced concrete beams. The results from the experimental and NLFEA were compared in terms of ultimate load, ultimate deflection, and the maximum strain induced in CFRP composites. The results obtained from the experimental tests are compared with the finite element analysis as shown in Figure 5. Inspection of Figure 5 reveals that the load-deflection curves from NLFEA had a good agreement with the experimental ones. Inspection of Figure 6 reflects that the NLFEA load-CFRP strain showed a little difference as compared with the experimental curves. Additionally, Table 1 reflected that the NLFEA can be considered as a mirror of experimental ones in terms of ultimate strength and corresponding deflection as well as mode of failure and crack patterns.

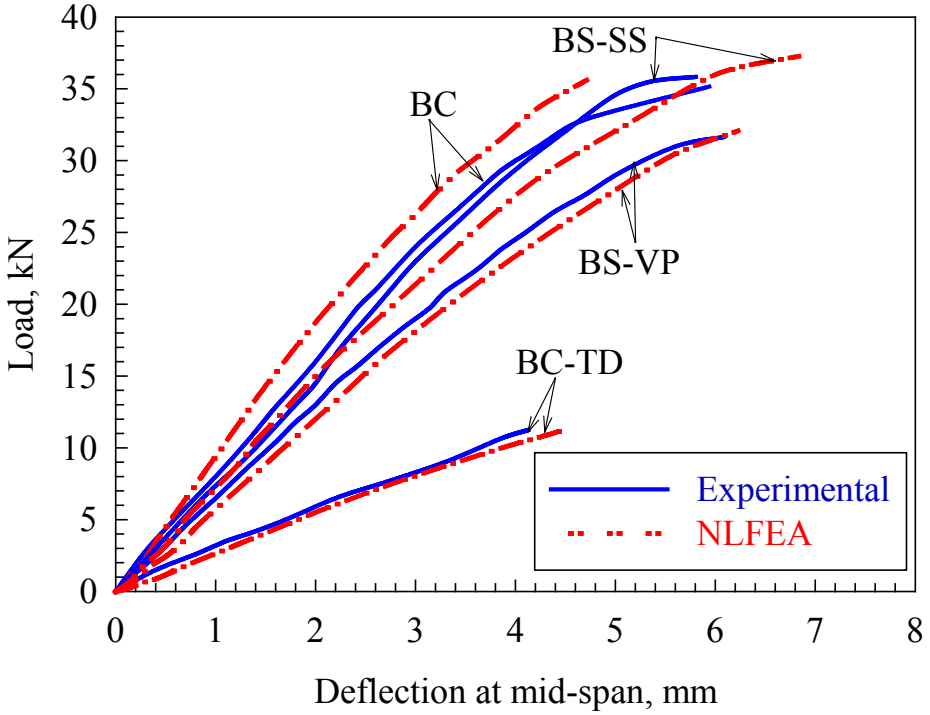

Figure 5. Experimental [48] and NLFEA load-deflection curves.

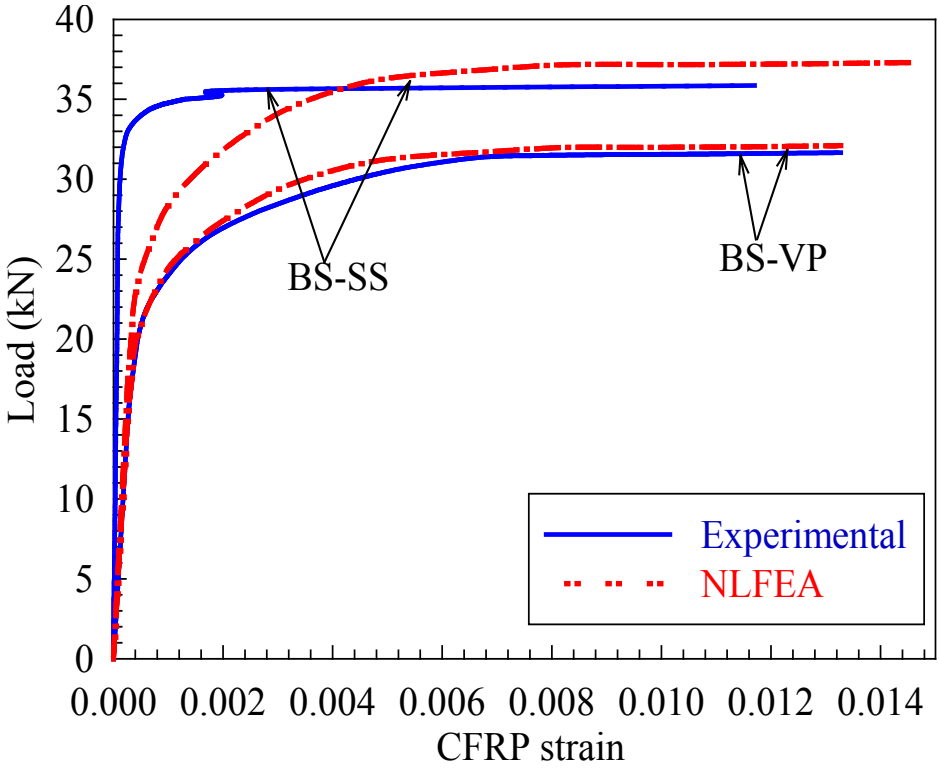

Figure 6. Experimental [48] and NLFEA CFRP strain curves.

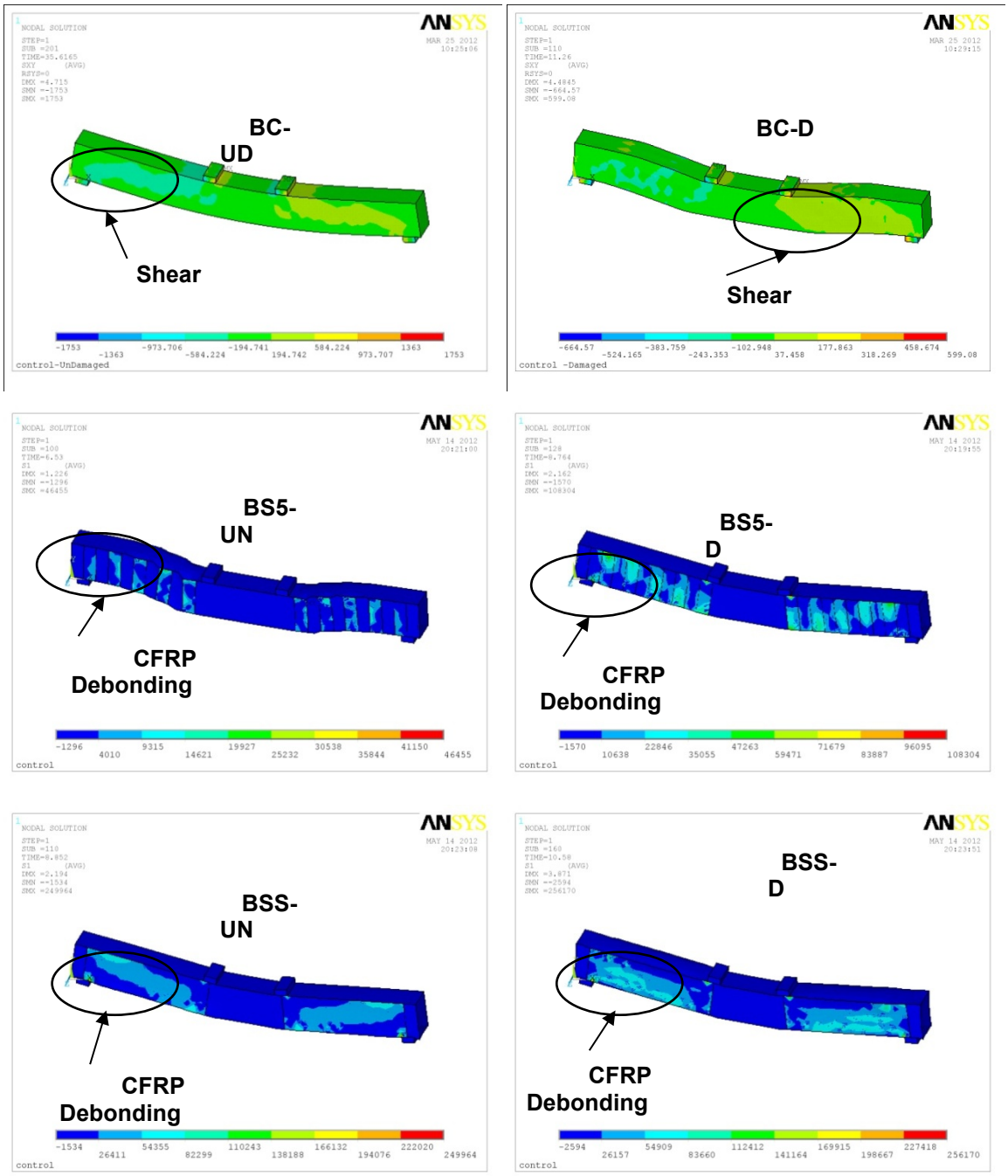

Figure 7. Typical NLFEA stress contours of undamaged, damaged, and strengthened beams.

3. Results and Discussion

3.1. Failure Mode

The trajectories of the stress obtained from the finite element analysis and modes of failure for control, damaged, and different strengthened RC beams are shown in Figure 7. A typical brittle shear failure was observed for control and damaged RC beams. The first flexural crack started within the constant moment region. As the load increased, cracks extended and additional flexural cracks developed throughout the beam length. An inclined shear crack was initiated close to the middle of the shear span. As the load increased, the shear crack propagated towards the loading and supporting points leading to a sudden brittle shear failure. Figure 7 shows the typical shear failure for control and damaged beams. Table 1 illustrated the cracking characteristics and modes of failure of different RC beams. The cracking patterns at failure for beams strengthened with vertical CFRP strips are shown in Figure 7. The strengthened beams showed less number cracks and large spacing as compared with control specimen. The flexural cracking load for beams strengthened with vertical and inclined CFRP plates were increased significantly to about 2 times that of control beams. The strengthened beams with fully sheet exhibited an initial flexural crack at the constant moment region. With further load increasing, the CFRP sheets rupture in the longitudinal direction of the fiber, after that the beam failed suddenly, no crack were visible on the shear span region due to the fully CFRP sheet. Also it can be noted that the use of fully CFRP plate was effective to delay the formation of the diagonal cracks and to arrest the propagation of the diagonal cracks than vertical CFRP ones.

Table 3. Results for all simulated models.

Group Number	Beam number	Ultimate deflection (mm)	Ultimate load (kN)	Elastic stiffness (kN/mm)	Toughness (kN.mm^2)	CFRP strain ($\mu\varepsilon$)	SF	DF	PF
1	BC-UD	4.7	35.6	9.2	95	---	1.00	1.00	1.00
	BS1-UD	5.8	46.3	9.7	153	12870	1.23	1.30	1.60
	BS3-UD	6.5	52.4	9.8	193	13580	1.38	1.47	2.03
	BS5-UD	7.1	57.0	9.7	230	14360	1.51	1.60	2.42
	BSS-UD	7.9	62.3	9.6	277	15010	1.66	1.75	2.91
2	BC-D	4.5	11.3	2.6	27	---	0.95	0.32	0.30
	BS1-D	5.4	23.1	4.9	69	12270	1.15	0.65	0.74
	BS3-D	5.8	27.3	5.4	87	13050	1.23	0.77	0.94
	BS5-D	6.2	32.1	5.9	110	13630	1.32	0.90	1.19
	BSS-D	6.8	37.3	7.2	152	14540	1.45	1.05	1.52

Note: SF: strength factor, DF: Ductility factor, PF: Performance Factor = SFxDF, STF: Stiffness Factor, ε_{CFRP} is the strain in CFRP strips and ε_{fu} is the ultimate strain in CFRP strips of 16400 $\mu\varepsilon$.

3.2. CFRP strain

Figure 8 shows the typical distribution of CFRP strain through the depth for all simulated beams. Inspection of Figure 8 reveals that the tensile stresses develop in the CFRP composites once the diagonal crack initiated in the concrete due to shear force. Furthermore, the maximum tensile stresses occurred close to the middle of the CFRP composite that intersect diagonal cracking near to the mid height of the beam cross section. Also, it is noticed that all simulated beams had CFRP strain below the maximum value of 16400 as shown in Table 3 and Table 4 as percentage of CFRP ultimate strain. Inspection of Table 4 reveals that the number of CFRP strips had a strong impact on the efficiency of CFRP strips for Group#1 (Un-Damaged) with a percentage with respect to ultimate strain of CFRP strips of 78 %, 83 %, 88 %, and 92 % for one, three, five, and fully strips, respectively. While, the percentage of Group#2(Damaged) with respect to ultimate strain of CFRP strips is 75 %, 80 %, 83 %, and 89 % for one, three, five, and fully stirrups, respectively, and this equivalent to 96 % of the Group 1 strains. In pre-cracking (diagonal shear crack) stage, CFRP strain development was equal to zero. After the creation of diagonal shear crack (the shear strength exceeds the concrete shear strength) within the shear span, the CFRP strain increased rapidly and continued to increase until the beam failure as shown in Figure 9. It can be observed that the strain in the CFRP developed at a low rate as the bond surface area decrease. Also the results indicated that the beams strengthened with fully CFRP sheet had highest impact on the CFRP strain.

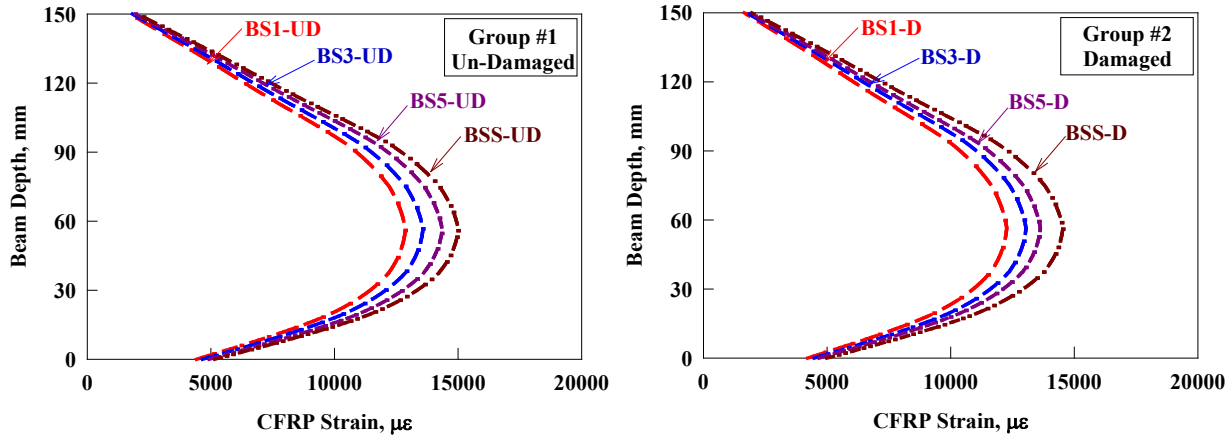

Figure 8. Typical CFRP strain versus beam depth.

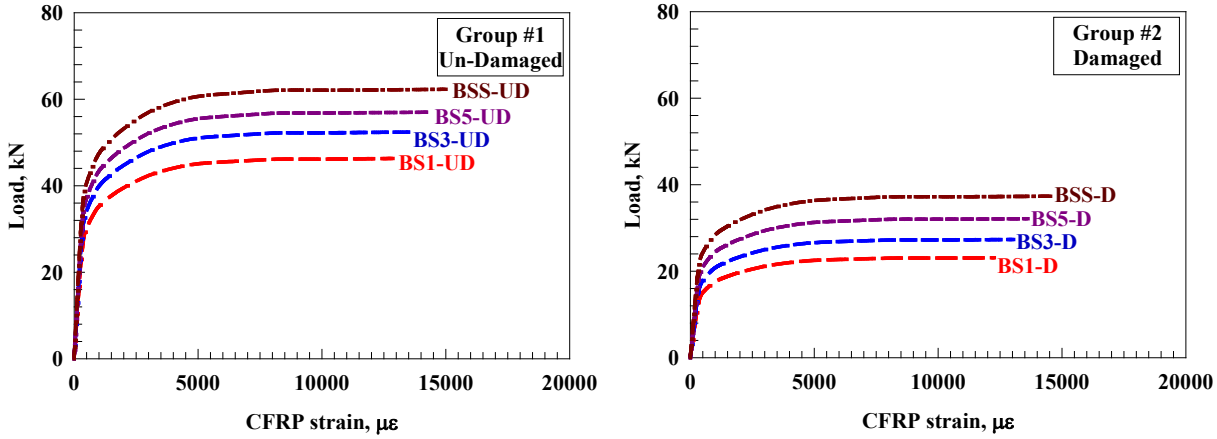

Figure 9. Typical load-CFRP strain curve.

Table 4. Percentage value of investigated parameters respect to control un-damaged beam.

Group Number	Beam	Ultimate deflection (%)	Ultimate load (%)	Performance factor (%)	Energy absorption (%)	Elastic stiffness (%)	ε_{CFRP}
1	BC-UD	0	0	0	0	0	–
	BS1-UD	23	30	60	6	60	$0.78\varepsilon_{fu}$
	BS3-UD	38	47	103	6	103	$0.83\varepsilon_{fu}$
	BS5-UD	51	60	142	6	142	$0.88\varepsilon_{fu}$
	BSS-UD	66	75	191	5	191	$0.92\varepsilon_{fu}$
2	BC-D	–5	–68	–70	–71	–72	–
	BS1-D	15	–35	–26	–47	–28	$0.75\varepsilon_{fu}$
	BS3-D	23	–23	–6	–42	–8	$0.80\varepsilon_{fu}$
	BS5-D	32	–10	19	–36	16	$0.83\varepsilon_{fu}$
	BSS-D	45	5	52	–22	60	$0.89\varepsilon_{fu}$

Note: ε_{fu} is the ultimate strain in CFRP strips of 16400 $\mu\varepsilon$.

3.3. Load-deflection behavior

Table 3 shows the characteristics of the load-deflection curves for control, thermal shock damage, and strengthened beams. The characteristics include the ultimate load capacity and the corresponding deflection at the mid-span, toughness, and stiffness. The initial stiffness is defined as the slope of linear elastic portion of beam at load-deflection curve ($k = P/\delta$). The toughness is defined as the area underneath the load-deflection curve until ultimate load capacity. The curves of load versus mid-span deflection can be divided into three specific regions: a linear elastic region up to first flexural crack, transition region up to the development of diagonal shear crack, and a post cracking region up to ultimate beam capacity as shown in Figure 10. Inspection of Figure 10 reveals that the load-deflection curve was extensively affected by thermal shock in terms of ultimate load, ultimate deflection, toughness, and stiffness as shown before in Table 3. The average ultimate load for control undamaged and damaged beams were 35.6 and 11.3 kN, respectively, with a percentage of reduction of about 68 %, as well as a reduction of 5 % in the ultimate deflection. In addition, the average stiffness for control undamaged and damaged beams were 9.2 and 2.6 kN/mm, respectively, with a reduction of 72 %, while the percentage of reduction in toughness was about 71 %. This significant reduction in ultimate load of damage beams is due to the reduction in compressive strength. In addition, the larger CFRP bonded area showed better performance than those with small CFRP bonded area.

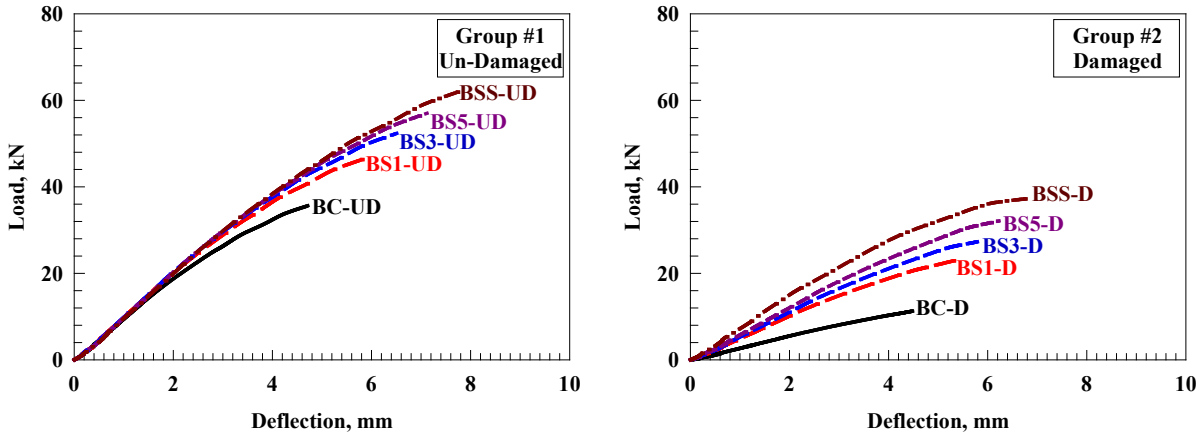

Figure 10. Typical load-deflection curve.

3.4. Ultimate load capacity and corresponding deflection

The assessment of beams for load capacity and corresponding deflection shows the excellent performance of RC members. For strengthened RC members, deflection and ultimate load capacity can be related to the serviceability and ultimate load limit states, respectively, as shown in Table 3. The load capacity and deflection percentages are defined as the ultimate load capacity and deflection, respectively, of CFRP strengthened beam divided by the ultimate deflection and load capacity of the un-strengthened beam (undamaged beam) as shown in Table 4. The deflection indicates how much the strengthened RC beams can sustain deformations without failure. The deflection percentage is defined as the ratio of the ultimate deflection of the strengthened beam to the ultimate deflection of the control beam (undamaged beam) as shown in Table 4. Strength ratio also predicts the increase of load that the model can sustain.

Figure 11 and 12 show the strength and ductility percentages with respect to un-damaged control beam, respectively, for all simulated models. Inspection of Figure 11 reveals that the strength percentage increased significantly with the increase of number of CFRP strips. The strength percentage (Figure 11) for Group #1 beams (Un-Damaged) is 30 %, 47 %, 60 %, and 75 % for beam strengthened with one, three, five and fully strips, respectively, with an significant average enhancement of 53 %. Also, the strength percentage (Figure 11) for Group #2 beams (Damaged) is –35 %, –23 %, –10 %, and 5 % for beam strengthened with one, three, five and fully strips, respectively,, with an significant average reduction of 16 % and this percentage is 0.25 times the percentage for Group#1 (Un-Damaged).

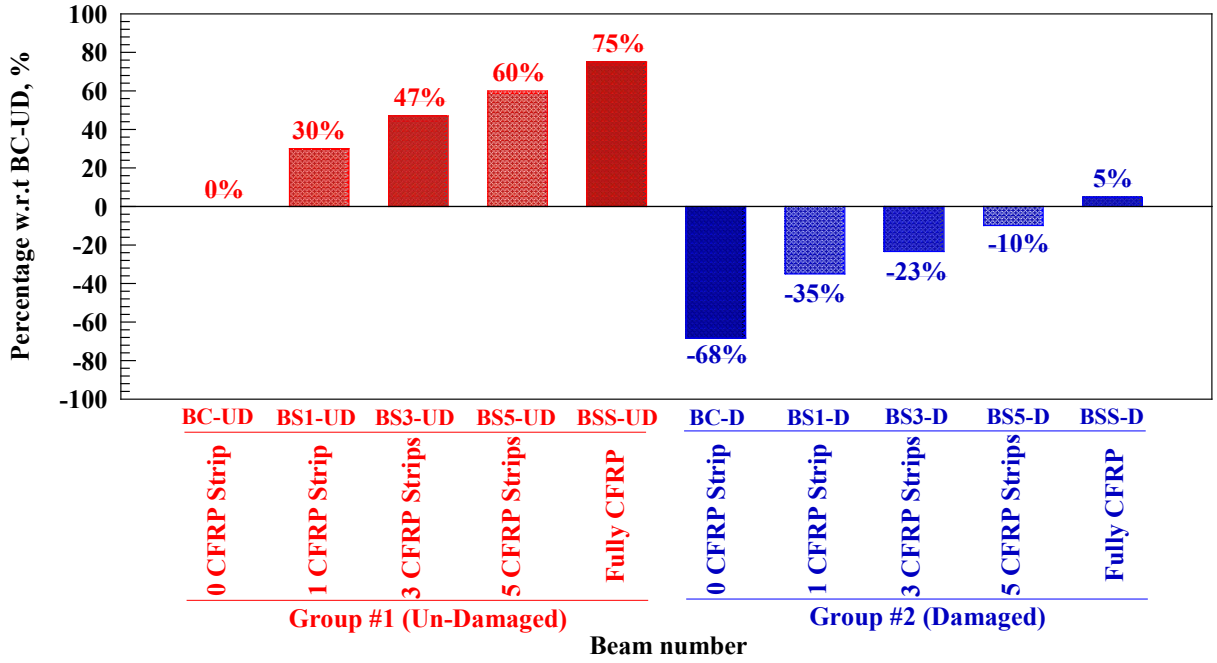

Figure 11. Ultimate load capacity percentage with respect to control undamaged beam

Figure 12 shows that the ductility percentage also significantly increased with the increase of number of CFRP strips. The ductility percentage (Figure 12) for Group #1 beams (Un-Damaged) is 23 %, 38 %, 51 %, and 66 % for beam strengthened with one, three, five and fully strips, respectively, with an significant average enhancement of 45 %. Also, the ductility percentage (Figure 12) for Group #2 beams (Damaged) is 15 %, 23 %, 32 %, and 45 % for beam strengthened with one, three, five and fully strips, respectively,, with an significant average enhancement of 29 % and this percentage is 0.64 times the percentage for Group#1 (Un-Damaged).

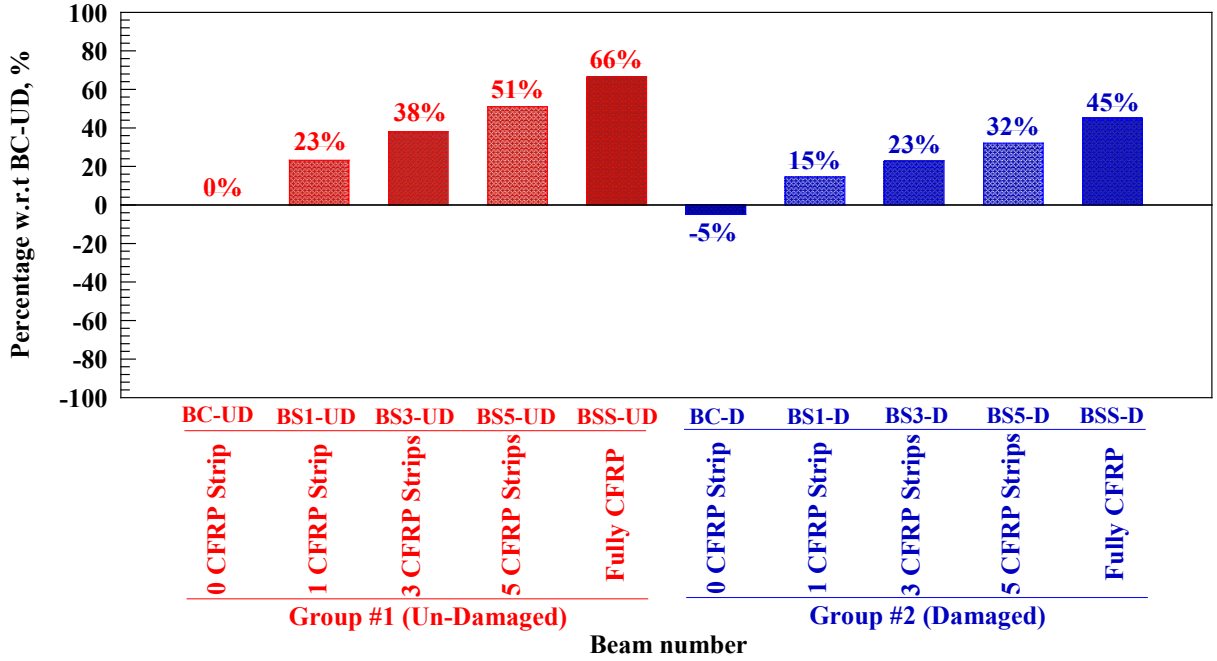

Figure 12. Ultimate deflection percentage with respect to control undamaged beam.

3.5. Elastic stiffness

The elastic stiffness determines the response of the crystal to an externally applied strain (or stress) and provides information about the bonding characteristics, mechanical and structural stability. The slope of the first stage of the load-deflection curve before initiation of the first main flexural crack is represented the elastic stiffness. For comparison, the elastic stiffness of each strengthened beam with CFRP sheets was normalized with respect to the control beam (Un-Damaged) without CFRP sheets as shown in Table 4.

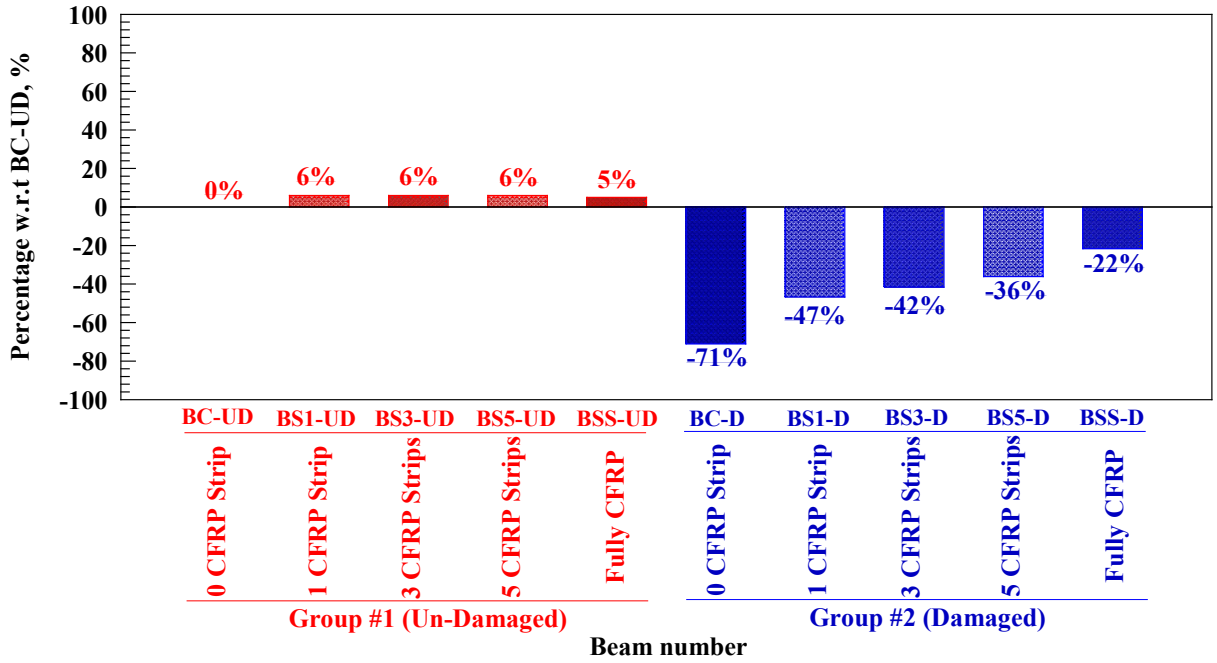

Figure 13. Stiffness percentage with respect to control undamaged beam.

Figure 13 shows the elastic stiffness percentages with respect to un-damaged control beam, respectively, for all simulated models. Inspection of Figure 13 reveals that the elastic stiffness percentage for un-damaged beams is the same for all strengthening techniques and equal to average value of 6 %. While, the elastic stiffness percentage for damaged beams is less than percentage of un-damaged beam and this value decreased with the increase of CFRP strips number. The elastic stiffness percentage (Figure 13) for Group #2 beams (Damaged) is –47 %, –42 %, –36 %, and –22 % for beam strengthened with one, three, five and fully strips, respectively, with an significant average reduction of 37 % and this percentage is eight times the percentage for Group#1 (Un-Damaged).

3.6. Toughness

In materials science and metallurgy, toughness is the ability of a material to absorb energy and plastically deform without fracturing. One definition of material toughness is the amount of energy per unit volume that a material can absorb before rupturing. Toughness is calculated as the entire area under the load-deflection curve. In addition, the toughness of each strengthened beam with CFRP sheets was normalized with respect to the control beams without CFRP sheets as shown in Table 4. Figure 14 shows that the toughness percentage also significantly increased with the increase of number of CFRP strips. The toughness percentage (Figure 14) for Group #1 beams (Un-Damaged) is 60 %, 103 %, 142 %, and 191 % for beam strengthened with one, three, five and fully strips, respectively, with an significant average enhancement of 124 %. Also, the toughness percentage (Figure 14) for Group #2 beams (Damaged) is –28 %, –8 %, 16 %, and 60 % for beam strengthened with one, three, five and fully strips, respectively, with an significant average enhancement of 10 % and this percentage is 0.08 times the percentage for Group#1 (Un-Damaged).

3.7. Evaluation of Performance of NLFEA Results

The effect of CFRP composite materials is evaluated by the strength factor (SF), deformability factor (DF), and performance factor (PF) for different strengthened RC beams normalized with respect to control beams (undamaged). Performance factor is a combination of the strength factor and the deformability factor to generate an overall structural performance as shown in Figure 15. Based on Figure 15 the DF, SF, and PF increased as the number of CFRP strips (bonded area of CFRP) increase. Finally, as the bonded area increase the beam reached the performance of control beams (undamaged) and protected the beams against brittle shear failure. The RC beams strengthened with fully CFRP sheet were much more effective in improving the performance of the strengthened beams than those beams strengthened with vertical strips. Thus, the beams strengthened with fully CFRP sheet is the most efficient technique than those strengthened with CFRP strips on the web.

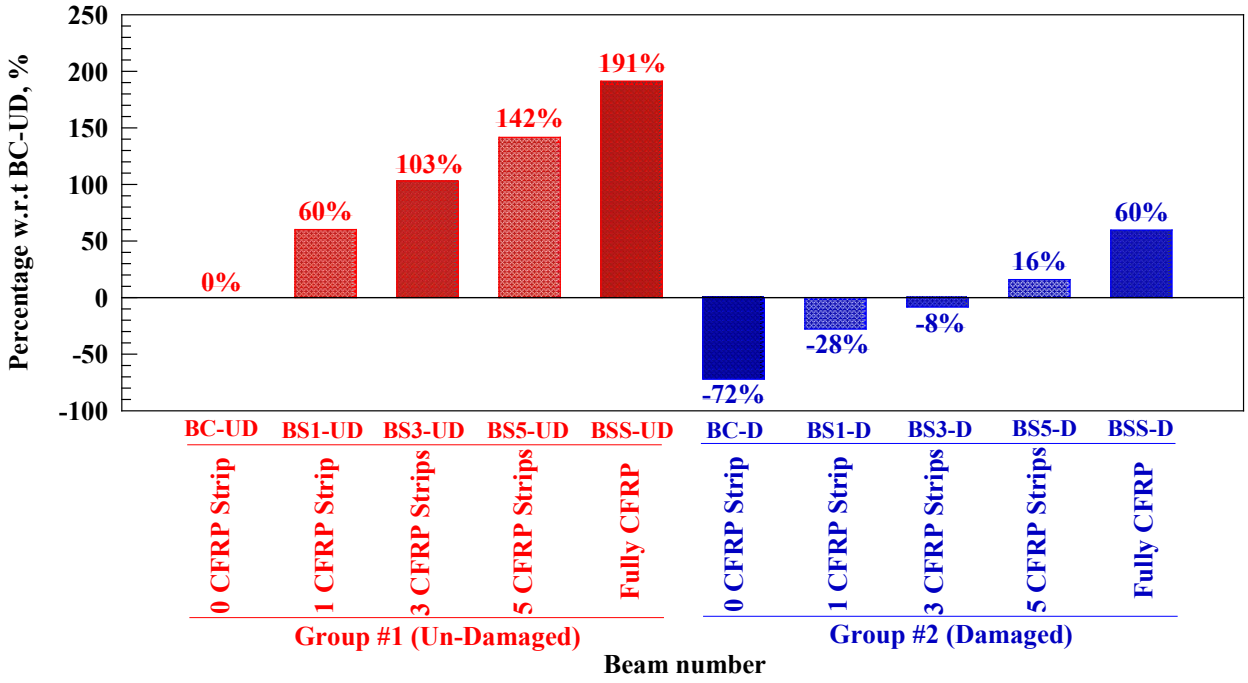

Figure 14. Toughness percentage with respect to control undamaged beam.

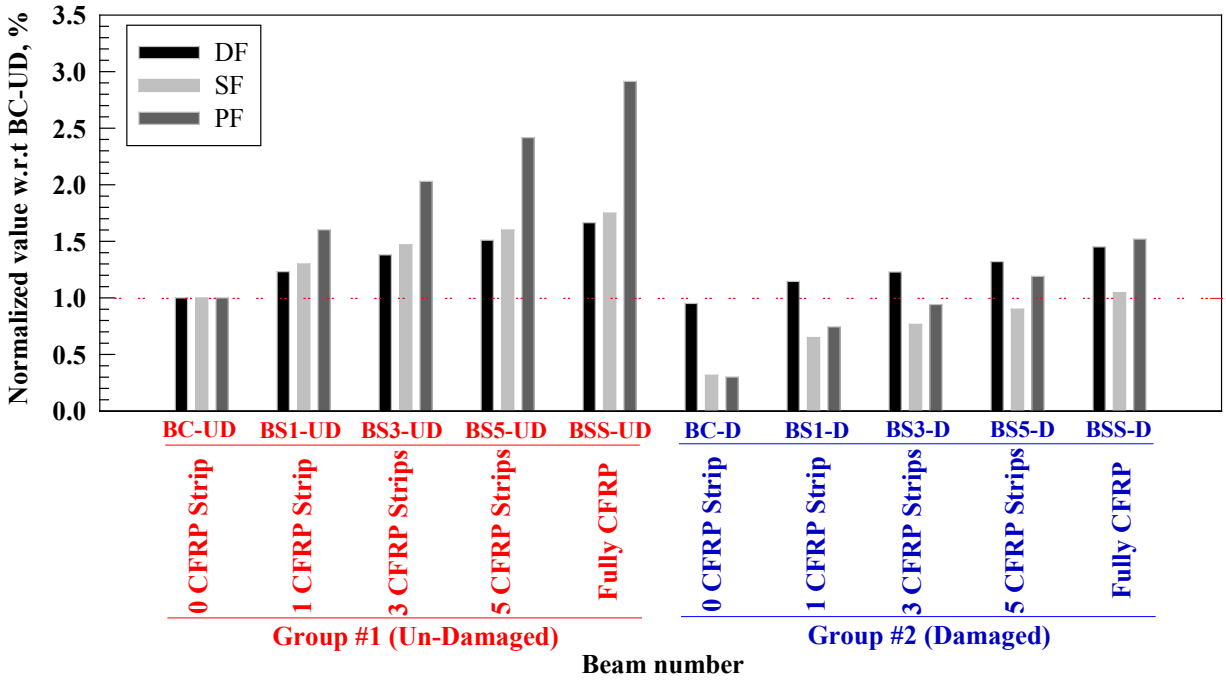

Figure 15. Normalized characteristic factor for different strengthened RC beams.

3.8. Profitability Index of the CFRP Strips Number

Table 5 shows the shear contribution of the concrete (V_c), shear contribution of the CFRP composites (V_f), and the final loads from the NLFEA for various RC beams strengthened using CFRP composites with different techniques. Table 5 indicated that the contribution of CFRP (V_f) to the shear capacity had increased as the CFRP bonded area increase or number of CFRP strips. To evaluate the efficiency of various CFRP composites strengthening techniques in terms of the amount of CFRP consumed, profitability indices were computed. The profitability index is defined as the ratio of CFRP contribution in shearing capacity to the total CFRP bonded area within the shear span of strengthened beams. Table 5 shows the profitability indices for the different strengthening techniques. Inspection of Table 5 reveals that the profitability index for undamaged beams were 3.57, 1.87, 1.43, and 0.99 MPa for 1, 2, 3, 4, and 9 CFRP strips (Fully), respectively. While, the profitability index for damaged beams were 3.93, 1.78, 1.39, and 0.96 MPa for 1, 2, 3, 4, and 9 CFRP strips (Fully), respectively, and these equivalent to 1.10, 0.95, 0.97, and 0.97, respectively, of the undamaged ones.

Table 5. Profitability index of CFRP strips.

Group Number	Beam number	V_c, kN	V_f, kN	V_u, kN	V_f/A_f, MPa
1	BC-UD	17.8	0.0	17.8	---
	BS1-UD	17.8	5.4	23.2	3.57
	BS3-UD	17.8	8.4	26.2	1.87
	BS5-UD	17.8	10.7	28.5	1.43
	BSS-UD	17.8	13.4	31.2	0.99
2	BC-D	5.7	0.0	5.7	---
	BS1-D	5.7	5.9	11.6	3.93
	BS3-D	5.7	8.0	13.7	1.78
	BS5-D	5.7	10.4	16.1	1.39
	BSS-D	5.7	13.0	18.7	0.96

Note: V_c is the shear contribution of the concrete, V_f is the shear contribution of the CFRP composites, A_f is the total CFRP bonded area within the shear span of strengthened beams

3.9. Comparison of NLFEA with other results

Comparison of NLFEA with Irshidat and Al-Saleh [51], the heat-damaged specimens repaired with FRP sheets based on neat epoxy (NE-500 and NE-600) experienced similar crack patterns of NLFEA. However, the presence of FRP sheet delayed the initiation of the flexural cracks in the area high moment zone. Specimen NE-500 was failed by sheet debonding followed by concrete crushing. The debonding started at the end of the specimen and extended to reach its center. Specimen NE-600 was failed by FRP sheet delaminating initiated at one end of the beam and extended toward the second end, followed by concrete crushing and splitting. Heating RC beams significantly affected their flexural behavior. Using externally bonded carbon fiber sheet/ epoxy composite to repair the heat-damaged RC beams help them to partially recover their flexural capacity is almost the same performance as the NLFEA.

4. Conclusions

1. NLFEA can be considered as a mirror of experimental ones in terms of ultimate strength and corresponding deflection as well as mode of failure and crack patterns. Hence, its results can be extended to generate data for cases, not studied experimentally.

2. NLFEA helped tracking propagation of cracks especially in case of beams externally strengthened with CFRP sheets in which crack patterns cannot be seen experimentally. The cracking patterns at failure as obtained from the NLFEA compared well with those observed experimentally for control, thermally damaged, and strengthened beams.

3. Subjecting thermal shock has a notable and significant impact on the mechanical properties and structural behavior represented in reduced shear capacity, stiffness, and toughness at percentages of 70 %, 72 % and 71 %, respectively, and formed extensive cracking in their concrete.

4. The beams strengthened with fully CFRP sheets achieved the highest load capacity, deflection, elastic stiffness, and toughness followed, in sequence, by those strengthened using five CFRP strips, three CFRP strips, one CFRP strip.

References

1. Kodur, A.V. The experimental behavior of FRP-strengthened RC beams subjected to design fire exposure. Engineering Structures. 2011. 33(1). Pp. 2201–2211. DOI: 10.1016/j.engstruct.2011.03.010.
2. Kodur, V.K.R., Agrawal, A. An approach for evaluating residual capacity of reinforced concrete beams exposed to fire. Engineering Structures. 2016. 110(1). Pp. 293–306. DOI: 10.1016/j.engstruct.2015.11.047.
3. Al-Ostaz, M. Irshidat, B. Tenkhoff, P.S. Ponnapalli. Deterioration of bond integrity between repair material and concrete due to thermal and mechanical incompatibilities. Journal of Materials in Civil Engineering. 2010. 22(2). Pp. 136–144. DOI: 10.1061/(ASCE)0899-1561(2010) 22:2(136).
4. Nedviga, E., Beresneva, N., Gravit, M., Blagodatskaya, A. Fire Resistance of Prefabricated Monolithic Reinforced Concrete Slabs of «Marko» Technology. Adv. Intell. Syst. Comput. 2018. 692(1): Pp. 739–749. DOI: 10.1007/978-3-319-70987-1_78.
5. Hezhev, T.A., Zhurtov, A.V., Tsipinov, A.S., Klyuev, S.V. Fire resistant fibre reinforced vermiculite concrete with volcanic application. Mag. Civ. Eng. 2018. 80(1). Pp. 181–194. DOI:10.18720/MCE.80.16.
6. Goremikins, V., Blesak, L., Novak, J., Wald, F. Experimental investigation on SFRC behaviour under elevated temperature. J. Struct. Fire Eng. 2017. 8(1). Pp. 287–299. DOI: 10.1108/JSFE-05-2017-0034.
7. Goremikins, V., Blesak, L., Novak, J., Wald, F. To testing of steel fibre reinforced concrete at elevated temperature. Appl. Struct. Fire Eng. 2017. DOI: 10.14311/asfe.2015.055.
8. Blesak, L., Goremikins, V., Wald, F., Sajdlova, T. Constitutive model of steel fibre reinforced concrete subjected to high temperatures. Acta Polytech. 2016. 56(1). Pp. 417–424. DOI: 10.14311/AP.2016.56.0417.
9. Goremikins, V., Blesak, L., Novak, J., Wald, F. Experimental method on investigation of fibre reinforced concrete at elevated temperatures. Acta Polytech. 2016. 56(1). Pp. 258–264. DOI: 10.14311/AP.2016.56.0258.

10. Selyaev, V.P., Nizina, T.A., Balykov, A.S., Nizin, D.R., Balbalin, A.V. Fractal analysis of deformation curves of fiber-reinforced fine-grained concretes under compression. PNRPU Mech. Bull. 2016. 1(1). Pp. 129–146. DOI: 10.15593/perm.mech/2016.1.09.
11. P. Bily, J. Fladr, A. Kohoutkova. Finite Element Modelling of a Prestressed Concrete Containment with a Steel Liner. Proceedings of the Fifteenth International Conference on Civil, Structural and Environmental Engineering Computing. Civil-Comp Press. 2015. DOI: 10.4203/ccp.108.1.
12. Bílý, P., Kohoutková, A. Sensitivity analysis of numerical model of prestressed concrete containment. Nucl. Eng. Des. 2015. 295(1). Pp. 204–214. DOI: 10.1016/j.nucengdes.2015.09.027.
13. Krishan, A., Rimshin, V., Erofeev, V., Kurbatov, V., Markov, S. The energy integrity resistance to the destruction of the long-term strength concrete. Procedia Eng. 2015. 117(1). Pp. 211–217. DOI: 10.1016/j.proeng.2015.08.143.
14. Korsun, V., Vatin, N., Franchi, A., Korsun, A., Crespi, P., Mashtaler, S. The strength and strain of high-strength concrete elements with confinement and steel fiber reinforcement including the conditions of the effect of elevated temperatures. Procedia Eng. 2015. 117(1). Pp. 970–979. DOI: 10.1016/j.proeng.2015.08.192.
15. Bily, P., Kohoutková, A. Numerical analysis of anchorage between steel liner and prestressed nuclear containment wall. Proc. 10th fib Int. PhD Symp. Civ. Eng. 2014. 529–534.
16. Korsun, V., Vatin, N., Korsun, A., Nemova, D. Physical-mechanical properties of the modified fine-grained concrete subjected to thermal effects up to 200°S. Appl. Mech. Mater. 2014. 633–634. Pp. 1013–1017. DOI: 10.4028/www.scientific.net/AMM.633-634.1013.
17. Korsun, V., Korsun, A., Volkov, A. Characteristics of mechanical and rheological properties of concrete under heating conditions up to 200°C. MATEC Web Conf. 2013. 6(1). Pp. 07002. DOI: 10.1051/matecconf/20130607002.
18. Petkova, T. Donchev, J. Wen. Experimental study of the performance of CFRP strengthened small scale beams after heating to high temperatures. Construction and Building Materials. 2014. 68(1): Pp. 55–61. DOI: 10.1016/j.conbuildmat.2014.06.014.
19. Ji, G., Li, G., Alaywan, W. A new fire resistant FRP for externally bonded concrete repair. Construction and Building Materials. 2013. 42(1). Pp. 87–96. DOI: 10.1016/j.conbuildmat.2013.01.008.
20. Trentin, J.R. Casas. Safety factors for CFRP strengthening in bending of reinforced concrete bridges. Composite Structures. 2015. 128(1). Pp. 188–198. DOI: 10.1016/j.compstruct.2015.03.048.
21. Ferrari, V.J., de Hanai, J.B., de Souza, R.A. Flexural strengthening of reinforcement concrete beams using high performance fiber reinforcement cement-based composite (HPFRCC) and carbon fiber reinforced polymers (CFRP). Construction and Building Materials. 2013. 48(1). Pp. 485–498. DOI: 10.1016/j.conbuildmat.2013.07.026.
22. Attari, N., Amziane, S., Chemrouk, M. Flexural strengthening of concrete beams using CFRP, GFRP and hybrid FRP sheets. Construction and Building Materials. 2012. 37(1). Pp. 746– 757. DOI: 10.1016/j.conbuildmat.2012.07.052 .
23. Kara, I.F., Ashour, A.F., Körog˘lu, M.A. Flexural behavior of hybrid FRP/steel reinforced concrete beams. Composite Structures. 2015. 129(1). Pp. 111–121. DOI: 10.1016/j.compstruct.2015.03.073.
24. Alver, N., Tanarslan, H.M., Sülün, Ö.Y., Ercan, E., Karcılı, M., Selman, E., Ohno, K. Effect of CFRP-spacing on fracture mechanism of CFRP-strengthened reinforced concrete beam identified by AE-SiGMA. Construction and Building Materials. 2014. 67(1). Pp. 146–156. DOI: 10.1016/j.conbuildmat.2014.05.017.
25. Khan, ur R., Fareed, S. Behaviour of reinforced concrete beams strengthened by CFRP wraps with and without end anchorages. Procedia Engineering. 2014. 77(1). Pp. 123–130. DOI: 10.1016/j.proeng.2014.07.011.
26. Hawileh, R.A., Rasheed, H.A., Abdalla, J.A., Al-Tamimi, A.K. Behavior of reinforced concrete beams strengthened with externally bonded hybrid fiber reinforced polymer systems. Mater. Des. 2014. 53(1). Pp. 972–982. DOI: 10.1016/j.matdes.2013.07.087.
27. You, Y.-C., Choi, K.-S., Kim, J. An experimental investigation on flexural behavior of RC beams strengthened with prestressed CFRP strips using a durable anchorage system. Composites Part B: Engineering. 2012. 43(1). Pp. 3026–3036. DOI: 10.1016/j.compositesb.2012.05.030.
28. Al-Rousan Rajai and Abo-Msamh Isra'a. Bending and Torsion Behaviour of CFRP Strengthened RC Beams. Magazine of Civil Engineering. 2019. 92(8). Pp. 62–71. DOI: 10.18720/MCE.92.8
29. Kiyanets, A.V. Concrete with recycled polyethylene terephthalate fiber. Magazine of Civil Engineering. 2018. 84(8). Pp. 109–118. doi: 10.18720/MCE.84.11.
30. Kolchunov, V.I., Dem'yanov, A.I. The modeling method of discrete cracks in reinforced concrete under the torsion with bending. Magazine of Civil Engineering. 2018. 81(5). Pp. 160–173. doi: 10.18720/MCE.81.16.
31. Travush, V.I., Konin, D.V., Krylov, A.S. Strength of reinforced concrete beams of high-performance concrete and fiber reinforced concrete. Magazine of Civil Engineering. 2018. No. 77(1). Pp. 90–100. doi: 10.18720/MCE.77.8.
32. Al-Rousan, R. Behavior of two-way slabs subjected to drop-weight. Magazine of Civil Engineering. 2019. 90(6). Pp. 62–71. DOI: 10.18720/MCE.90.6
33. Al-Rousan, R. The impact of cable spacing on the behavior of cable-stayed bridges. Magazine of Civil Engineering. 2019. 91(7). Pp. 49–59. DOI: 10.18720/MCE.91.5
34. Yu, V.K.R. Kodur. Fire behavior of concrete T-beams strengthened with nearsurface mounted FRP reinforcement. Engineering Structures. 2014. 80(1). Pp. 350–361. DOI: 10.1016/j.engstruct.2014.09.003.
35. Khan, M.S., Prasad, J., Abbas, H. Shear strength of RC beams subjected to cyclic thermal loading. Construction and Building Materials. 2010. 24(10). Pp. 1869–1877. DOI: 10.1016/j.conbuildmat.2010.04.016
36. Xiangwei, Liang, Chengqing, Wu, Yekai, Yang, Cheng, Wu, Zhongxian, Li. Coupled effect of temperature and impact loading on tensile strength of ultra-high performance fibre reinforced concrete. Composite Structures. 2019. 229(1). Pp. 111432. DOI: 10.1016/j.compstruct.2019.111432.
37. Bingol, A.F., Gul, R. Effect of elevated temperatures and cooling regimes on normal strength concrete. Fire and Materials. 2009.33(1). Pp. 79–88. DOI: 10.1002/fam.987
38. Lu, X.Z., Chen, J.F., Ye, L.P., Teng, J.G., Rotter, J.M. RC beams shear-strengthened with FRP: Stress distributions in the FRP reinforcement. Construction and Building Materials. 2009. 23(1). Pp. 1544–1554. DOI: 10.1016/j.conbuildmat.2008.09.019
39. Jiangfeng Dong, Qingyuan Wang, and Zhongwei Guan. Structural behaviour of RC beams with external flexural and flexural–shear strengthening by FRP sheets. Composites Part B: Engineering. 2013. 44(1). Pp. 604–612. DOI: 0.1016/j.compositesb.2012.02.018
40. Ahmed K. El-Sayed. Effect of longitudinal CFRP strengthening on the shear resistance of reinforced concrete beams. Composites Part B: Engineering. 2014. 55(1). Pp. 422–429. DOI: 10.1016/j.compositesb.2013.10.061

41. Carlo Pellegrino and Mira Vasic. Assessment of design procedures for the use of externally bonded FRP composites in shear strengthening of reinforced concrete beams. Composites Part B: Engineering. 2013. 45(1). Pp. 727–741. DOI: 10.1016/j.compositesb.2012.07.039
42. Davood Mostofinejad and Amirhomayoon Tabatabaei Kashani. Experimental study on effect of EBR and EBROG methods on debonding of FRP sheets used for shear strengthening of RC beams. Composites Part B: Engineering. 2013. 45(1). Pp. 1704–1713. DOI: 10.1016/j.compositesb.2012.09.081
43. Marco Corradi, Antonio Borri, Giulio Castori, and Romina Sisti. Shear strengthening of wall panels through jacketing with cement mortar reinforced by GFRP grids. Composites Part B: Engineering. 2014. 64(1). Pp. 33–42. DOI: 10.1016/j.compositesb.2014.03.022
44. Dias, S.J.E., Barros, J.A.O. NSM shear strengthening technique with CFRP laminates applied in high-strength concrete beams with or without pre-cracking. Composites Part B: Engineering. 2012. 43(2). Pp. 290–301. DOI: 10.1016/j.compositesb.2011.09.006
45. Massimiliano Bocciarelli, Serena Gambarelli, Nicola Nisticò, Marco Andrea Pisani, and Carlo Poggi. Shear failure of RC elements strengthened with steel profiles and CFRP wraps. Composites Part B: Engineering. 2014. 67(1). Pp. 9–21. DOI: 10.1016/j.compositesb.2014.06.009
46. Sheikh, S.A. Performance of concrete structures retrofitted with fiber reinforced polymers. Engineering Structures. 2002. 24(7). Pp. 869–879. DOI: 10.1016/S0141-0296(02)00025-1
47. Liu, F., Wu, B., Wei, D. Failure modes of reinforced concrete beams strengthened with carbon fiber sheet in fire. Fire Safety Journal. 2009. 44(7). Pp. 941–950. DOI: 10.1016/j.firesaf.2009.05.006
48. Rajai Z. Al-Rousan, Rami H. Haddad, Alaa O. Swesi. Repair of shear-deficient normal weight concrete beams damaged by thermal shock using advanced composite materials. Composites Part B: Engineering. 2015; 70(1). Pp. 20–34. DOI: 10.1016/j.compositesb.2014.10.032.
49. Zhang, Y.X., Bradford, M.A. Nonlinear analysis of moderately thick reinforced concrete slabs at elevated temperatures using a rectangular layered plate element with Timoshenko beam functions. Engineering Structures. 2007. 29(10). Pp. 2751–2761. DOI: 10.1016/j.engstruct.2007.01.016
50. Rami H. Haddad, Rajai Z. Al-Rousan. An anchorage system for CFRP strips bonded to thermally shocked concrete. International Journal of Adhesion and Adhesives. 2016. 71(1). Pp. 10–22. DOI: 10.1016/j.ijadhadh.2016.08.003
51. Mohammad, R. Irshidat, Mohammed H. Al-Saleh. Flexural strength recovery of heat-damaged RC beams using carbon nanotubes modified CFRP. Construction and Building Materials. 2017. 145(1). Pp. 474–482. DOI: 10.1016/j.conbuildmat.2017.04.047.

Contacts

Rajai Al-Rousan, rzalrousan@just.edu.jo